Preprint
UCRL-JC-135554

A Comparison of Spectroscopic Measurements of an Inductive Plasma Source with the INDUCT Model

M.L. Huebschman, V. Bakshi, R.D. Bengston, J.G. Ekerdt, P.A. Vitello, J.C. Wiley, N. Xiang

This article was submitted to
46th International Symposium of the American Vacuum Society,
Seattle, WA, October 25-29, 1999

October 3, 1999

U.S. Department of Energy
Lawrence Livermore National Laboratory

A comparison of spectroscopic measurements of an inductive plasma source with the INDUCT model.

M. L. Huebschman.[1,2], V. Bakshi[2], Roger D. Bengtson[1], J. G. Ekerdt[1], P. A. Vitello[3], J. C. Wiley[1], and N. Xiang[1]

[1] The University of Texas at Austin
Austin, TX 78712 USA

[2] Sematech International
Austin, TX 78741 USA

[3] Lawrence Livermore National Laboratory
Livermore, CA

Abstract

Noninvasive spectroscopic measurements of an inductively driven hydrogen plasma source with density and temperature characteristic of plasma processing tools have been made with an ultimate application of cleaning of silicon substrates These measurements allow full radial and axial profiles of electron density and temperature to be measured from absolutely calibrated multichannel spectroscopic measurements of upper state number densities and a collisional radiative model. Profiles were obtained over a range of powers from 50 to 200 W and pressures from 5 to 50 mTorr in hydrogen in a small cylindrical source. The hydrogen working gas and simple cylindrical geometry was chosen to simplify detailed comparisons with a 2D computational model (INDUCT95) which uses a fluid approximation for the plasma and neutral gas. The code calculates the inductive coupling of the 13.56 MHz RF source, the collisional, radiative, and wall losses as well as a chemistry model for electrons, H_2, H, H^+,H_2^+, and H_3^+. Simulation results were sensitive to the value for the wall coefficient. The simulation and experimental temperature and density profiles in r and z were in rough agreement, but some details were quite different. The simulated axial density profile was located under the coil while the measured density profiles extended well beyond the edges of the coil. The scaling of conditions with pressure and power was in rough agreement between experiment and simulations.

I. Introduction

A number of studies[1-6] have shown that hydrogen plasmas can be used to clean the silicon surface of carbon and halogen impurities, etch the native oxide, and passivate the cleaned surface with adsorbed hydrogen. Critical to advancing plasma based cleaning processes is a first principles based model, that can be verified by accurate measurements in the plasma, and which couples the surface reactions resulting from the incident neutral species (H) and ions (H^+) to a rigorous description of the phenomena occurring in the plasma. As a first step in a detailed model verification, we have chosen the simplest chemical system, pure hydrogen, in a simple cylindrical geometry where we measured plasma conditions using noninvasive spectroscopic diagnostics and compared these measurements with a model based on INDUCT-95[7] using a minimum of geometric boundary conditions. Even this greatly simplified reactor presents complex challenges both experimentally and numerically which need to be understood before more commercially relevant reactors can be modeled with confidence.

In the following section we describe the experiment, the collisional radiative model[8] and the procedures for obtaining electron temperature and density profiles from the spectroscopic measurements. We then describe the fluid model, using INDUCT-95, that we used to model the power deposition, transport, and chemistry. In the last section we compare the model predictions with measurements.

II. Description of experiment

The plasma was created in a quartz cylinder (2 cm radius, 75 cm length) attached to a stainless steel vacuum chamber with a base pressure less than 1×10^{-9} Torr with a 15 turn coil surrounding the cylinder. The power source is a 500 W, 13.6 MHz supply with impedance matching to match the source to the plasma load. The power meter was used to measure power from the source with a reflected power that was always less than 1%. Pressure of the slowly flowing hydrogen gas was varied from 5 to 50 mTorr over a range of power from 50 W to 200 W. Details of the source are given in reference 9.

In order to maintain cleanliness in the plasma we chose to use noninvasive, nonperturbing spectroscopic techniques. Local plasma conditions were measured using an 18 channel, fiber optic input monochromater with a 384 by 576 detector array. Using this system we measured eight hydrogen line intensities on 18 chords at a single axial position in about 5 minutes. We saw several weak features in the spectra that could be identified as molecular hydrogen. We saw no spectral features that could be clearly identified as impurities. We measured up to 14 independent positions along the plasma axis at each operating condition. These data were then Abel inverted to convert the line integrated measurements to local intensities or upper state number densities of up to eight levels with a spatial resolution of order 2 mm in both radial and axial dimensions within the cylindrical plasma. The entire spectroscopic system was absolutely

calibrated using a tungsten filament source[10] operating at conditions that could be traced back to the National Bureau of Standards. We estimate the calibration accuracy over the entire spectral range to be accurate to ±14%. Figure 1 shows typical data for one position located in r and z. Note that we have measurements of the upper states from p = 3 to p =12 but did not include p = 8, 9, and 11 in our analysis because of interference with hydrogen molecular lines.

Using the local measurements of upper state number density of several lines, we calculated a local electron temperature and density by minimizing the rms deviation between the measured populations and calculated populations from a collisional-radiative model by Sawada and Fujimoto[8]. The collisional-radiative model incorporates collisions, and radiative transitions between atomic states, recombination from free electrons to bound atomic states, and dissociation from molecular hydrogen or molecular hydrogenic ions to populate the levels in the hydrogen atom. That is, the gain-loss equations for the atomic levels are closed with an assumption of local thermal equilibrium for atomic levels greater than 40. All of the rates used have an assumption of a Maxwellian electron distribution. The atomic and molecular rates used in the data reduction are the rates given in reference 8. It should be pointed out that the atomic rates and transition probabilities for hydrogen are well known compared to any other atom or molecule, thus facilitating both the diagnostics and the simulation. An additional input is the pressure of the system which was measured by a pressure gauge well away from the plasma. For an electron temperature, T_e, and density, n_e, the collisional-radiative model defines a set of effective population coefficients and rate coefficients. The atomic and molecular ground state densities are then determined from the total pressure, ionization and recombination rates for hydrogen and a dissociation rate for molecular hydrogen. We assumed the molecular hydrogen to be at room temperature, and took the temperature of hydrogen atoms and protons to be 0.1 eV, a temperature consistent with the observed line widths which were slightly larger than our instrumental line profile. Minimizing the standard deviation in the least squares fit to the data was a sensitive definition of T_e and n_e. Varying measured inputs over the 14% uncertainty from calibration and Abel inversion gives an error estimate of 3.3% for T_e and15% for n_e. While our data analysis using the collisional radiative model provides an estimate of molecular hydrogen density, we do not have a direct absolute measure of molecular density and will not compare experimental and simulation results for molecular density. In retrospect, a direct measure of molecular composition is an important parameter for an experimental/simulation comparison.

In fitting of upper state populations to obtain electron temperature and density it is important to measure and fit to as many upper state populations as possible to minimize experimental uncertainties in calibration and to avoid uncertainties with recombining and ionizing plasmas. A typical fit of measured upper state densities to the

C-R model is shown in figure 1. Note that the upper state populations scale as p^4 rather than as $e^{-\Delta E/kT}$. Details of the experiment can be found in reference 11.

III. Description of Induct-95

The computational model is based on a code developed by P. A. Vitello et. al[7]. We are using version INDUCT-95.6. We have installed a new geometry model that describes the cylindrical inductive plasma and have added chemical reactions and rates to describe the hydrogen chemistry. INDUCT-95 includes a version of ORMAX[12] which solves the time averaged Maxwell's equations which connect the plasma with the RF currents flowing in the coil. The ions are modeled using continuity and momentum conservation equations. The continuity equation for the ion species i is

$$\frac{\partial n_i}{\partial t} = -\vec{\nabla} \bullet n_i \vec{v}_i + \sum_{j=1}^{N_c} R_{i,j}, \tag{1}$$

where $R_{i,j}$ is the chemical reaction generating ions i from reaction j, and N_c is the total number of chemical reactions. The reactions for the hydrogen chemical model include ionization, recombination, excitation and dissociation. The ion momentum balance equation is

$$\frac{\partial n_i \vec{v}_i}{\partial t} = -\vec{\nabla} \bullet n_i \vec{v}_i \vec{v}_i + \frac{q_i n_i \vec{E}}{m_i} - \frac{\vec{\nabla} n_i k T_i}{m_i} - \sum_{j=1}^{N_N} n_i \nu_i \nu_{i,j}, \tag{2}$$

where N_N is the total number of neutral species. The ion-neutral collision frequency is given by

$$\nu_{i,j} = \sigma_{i,j} v_i n_j, \tag{3}$$

where σ_{ij} is the ion neutral cross-section between ion species i and neutral species j with density n_j. The relative velocity is computed from

$$\bar{v}_i = \left(\frac{3kT_i}{m_i} + \vec{v}_i \bullet \vec{v}_i \right)^{1/2}, \tag{4}$$

The electrons are modeled using the electron continuity equation

$$\frac{\partial n_e}{\partial t} = -\vec{\nabla} \bullet \vec{\Gamma}_e + \sum_{j=1}^{N_c} R_{e,j}, \tag{5}$$

where $R_{e,j}$ is the chemical reaction rate generating electrons from reaction j, and N_C is the total number of chemical reactions.

The electron energy balance equation is

$$\frac{\partial W_e}{\partial t} = -\vec{\nabla} \bullet \vec{Q} - e\vec{\Gamma}_e \bullet \vec{E} + P_{ind} - P_{coll}, \tag{6}$$

where the electron flux uses the "drift-diffusion" approximation

$$\vec{\Gamma}_e = -n_e \mu_e \vec{E} - \frac{1}{m_e \nu_N} \vec{\nabla} n_e k T_e, \tag{7}$$

and the heat flux is given by

$$\vec{Q} = \frac{5}{2}\vec{\Gamma}_e kT_e - \frac{5}{2}\frac{n_e kT_e}{m_e \nu_N}\nabla(kT_e), \tag{8}$$

with $W_e = 3n_e kT_e/2$ and the electron mobility, $\mu_e = |q|/m\nu$. The P_{ind} term is found from the time averaged Maxwell's equations for the coil-plasma system using the ORMAX formulation.

The electric potential is calculated self-consistently through Poisson's equation

$$\vec{\nabla} \bullet \varepsilon \vec{\nabla}\phi = -\left(\sum_{i=1}^{N_i} q_i n_i + q_e n_e\right), \tag{9}$$

where ε is the local dielectric constant.

The neutral particles are treated assuming a spatially averaged constant total pressure and a uniform neutral temperature. In the results presented here a constant neutral temperature of 0.05 eV was assumed, somewhat above room temperature but consistent with the collisional radiative model used to interpret the data. The neutral continuity equations are used to calculate number densities

$$\frac{\partial n_n}{\partial t} = -D_n \nabla^2 n_n + \sum_{j=1}^{N_C} R_{n,j}. \tag{10}$$

The computational domain represents a cylindrically symmetric region 5 cm in radius and 50 cm long divided into a rectangular mesh 101 x 41. There is one mesh for the fluid calculation and one for the RF heating. In keeping with the philosophy of making a geometrically and chemically simple system, the simulation includes only a quartz tube, the coils, and a surrounding non plasma region. While in the experiment there is a small hydrogen inflow, the rate is slow enough it can be neglected on the simulation time scales allowing the inflow and pumped boundary conditions to be neglected. The experiment is modeled as a closed container with the wall reactions operating on all surfaces. Note that the fluid simulation geometry is close to the experiment, but not identical. To make the fluid simulation match the dimensions of the experiment with the detail level of the experiment would have required a larger grid and a significantly longer run time. Even with these simplifications a typical simulation for one experimental condition requires from 10 to 20 hours with a 400 MHz PC.

The reactions for the hydrogen chemical model include dissociation, ionization, recombination, and excitation. The six species used in this model are e, H^+, H_2^+, H_3^+, H_2, and H. The chemical reactions considered in the fluid and the references for the reaction rates are shown in Table I. In general we used the same reaction rates as were used in the collisional radiative model for determining temperature and density. The simulations required more rates than for our collisional radiative diagnostic analysis because we included an additional species H_3^+ in the simulations. The additional rates can be found in references 13 and 14. We have not included the negative ion H^- in our simulations because at the electron temperatures observed, the number density of H^- was small.

The wall reactions used in the simulation are shown in table II. The simulation results were sensitive to the value for the wall coefficient for the reaction H + Wall—> 1/2 H_2. The large surface/volume ratio in this simulation means that collisions with the walls are quite likely. When two hydrogen atoms create a molecule at the wall, it requires significantly more energy to dissociate the molecule back to atoms and reduces the plasma temperature. For our most studied case [200 W power into 50 mTorr] a change from a wall coefficient from $5x10^{-4}$ to 10^{-3} reduced the peak electron temperature by 11% and increased the average electron density by about 15%. We used a wall coefficient of 2×10^{-3} for all comparisons between simulations and experiment because it gave the best comparision between measurements and simulations. The ratio of hydrogen molecules to atoms is sensitive to the wall coefficient and additional measurements of the molecular state would be useful in defining a wall coefficient.

IV. Comparison between experiment and simulation

In this comparison we will compare only directly measured quantities; that is, we will compare the electron density and temperature measurements from the experiment with the simulations. We have measured the intensity of molecular features in our spectra but have not been able to estimate a molecular density from these measurements. A direct measure of atomic and molecular density would be a good check on wall contributions. To simulate the 200 W power from the source in the experiment we have estimated a power loss in the coil and leads of 10%.

In figure 2 we show radial profiles of electron temperature and density near the center of the coil coming from the Abel inversion procedure of 18 line averaged intensities for 50 mTorr pressure and 200 W power along with profiles from the simulations. While there is a significant difference in the peak value of the density profile, probably from slightly different axial positions, the experimental and simulated profile shapes are very similar.

In figure 3 we present axial profiles of the electron density from experiment and simulation for the same conditions as figure 2. We were limited to 7 axial positions experimentally because of conflicts between coils and optical apparatus. We have aligned the experimental and simulation data around the center of the coil. Note that the profiles are not symmetric about the center of the coil, and that the simulation profiles and experimental profiles are not asymmetric in the same way. We attribute this difference to differences in the boundary conditions. In the experiment, the plasma cylinder end went into a large vacuum chamber held at constant pressure. The plasma cylinder was terminated with a wall in the simulations. The most apparent difference in the experimental and simulation profiles is that the electron density profile does not extend beyond the edges of the coil while the experimental profile fills the entire cylinder.

In figure 4 we compare experiment and simulation as a function of power. Because of the difference in electron temperature and density profiles between conditions and between experiment and simulation we have averaged the temperatures and densities for both simulation and experiment over the volume of the plasma surrounded by the coil. This was an arbitrary choice and there may be may ways of looking at scaling. For the two conditions shown in figure 4, the scaling with power for the experiment and simulations seems to show crude agreement. We used the same wall coefficients for high power and low power simulations.

In figure 5 we compare experiment and simulations as a function of gas pressure. Again the scalings are suggestive, but the caveats about the power scaling hold for this comparison also. At the lower pressures of this experiment, the fluid model may be suspect. Simulations so far do not show the limitations of the fluid model. While these comparisons between theory and experiment look quite promising, further and more detailed work is needed.

V. Conclusions

We have compared electron temperature and density measurements from non perturbing spectroscopic diagnostics with simulations from the INDUCT-95 fluid code. The simulations were quite sensitive to the wall coefficients. A comparison of the details of the temperature and density profiles between the experiments and simulations showed significant differences while the broad features agreed well. Scalings with pressure and power were in agreement despite significant differences in profiles. With this simple geometry and relatively well defined atomic rates, the large features of experiment and simulation were in reasonable agreement. Further work will concentrate on a closer comparison of the measurements and simulations.

This work was supported in part by grant # ARP-436 from the Texas Advanced Research Program to The University of Texas at Austin and in part under the auspices of the U.S. Department of Energy at Lawrence Livermore National Laboratory under Contract W-7405-ENG-48.

References

1. W. Hansch, *et al.*, Jpn. J. Appl. Phys. **33**, 2262 (1994).
2. R. P. H. Chang, C. C. Chang, S. Darack, J. Vac. Sci. Techol. A **20**, 45 (1982).
3. R. J. Carter, T. P. Schneider, et al, J. electrochemj. Soc. **141**, 3136 (1994)
4. A. Kishimoto, *et al.*, Jpn. J. Appl. Phys. **29**, 2273 (1990).
5. J. Ramm, E. Beck, *et al.*, Thin Solid Film **246**, 158 (1994)
6. Y. Saito, Appl. Surf. Sci. **81**, 223 (1994).
7. PJ. A. Vitello, R. A. Stewart, *et al.* UCRL-MA120465, March 1995.
8. Sawada and T. Fujimoto, J. Appl. Phys. **78**, 5 (1995). See also T. Fujimoto, K. Sawada, and Takahata., J. Appl. Phys. **66**, 6 (1989).
9. G. M. Sampson, J. M. White, J. G. Ekerdt, Applied Surface Science, **143**, 30 (1990)
10. R. Stair, R. G. Johnston, and E. W. Halbach, Journal of Research of NBS, A. **64A**, 291, (1960).
11. Michael Huebschmann, Dissertation, The University of Texas at Austin, (1999).
12. E. F. Jaeger, L. A. Berry, *et al.* Phys. Plasmas. **2**, 2597 (1995).
13. R. K. Janev, et.al. *Elementary Processes in Hydrogen-Helium Plasmas*, Springer-Verlag, (1987).
14. M. A. Lieberman, A. J. Lichtenberg, *Principles of plasma discharges and materials processing*, John Wiley & Sons, Inc. (1994).

Figure Captions

1. Comparision of upper state populations measured from experiment(O) with the best fit from the collisional radiative model (+) as a function of principle quantum number p. The electron temperature and density from this fit is $T_e = 3.5$ eV and $n_e = 3.4 \times 10^{10}$ cm^{-3}.

2. (a) Radial profiles of electron temperature from experiment and simulation.

(b) Radial profiles of electron density from experiment and simulation. Both profiles were taken near the center of the coil. Conditions are 200 W input power, 50 mTorr pressure.

3. (a) Electron temperature axial profiles from experiment and simulation.

(b) Electron density axial profiles from experiment and simulation. Conditions are 200 W power and 50 mTorr pressure.

4. (a) Average temperature under the coil from experiment and simulation as a function of power.

(b) Average density under coil from experiment and simulation as a function of power.

5. (a) Average temperature under the coil from experiment and simulation as a function of pressure.

(b) Average density under coil from experiment as simulation as a function of pressure.

Figure 1

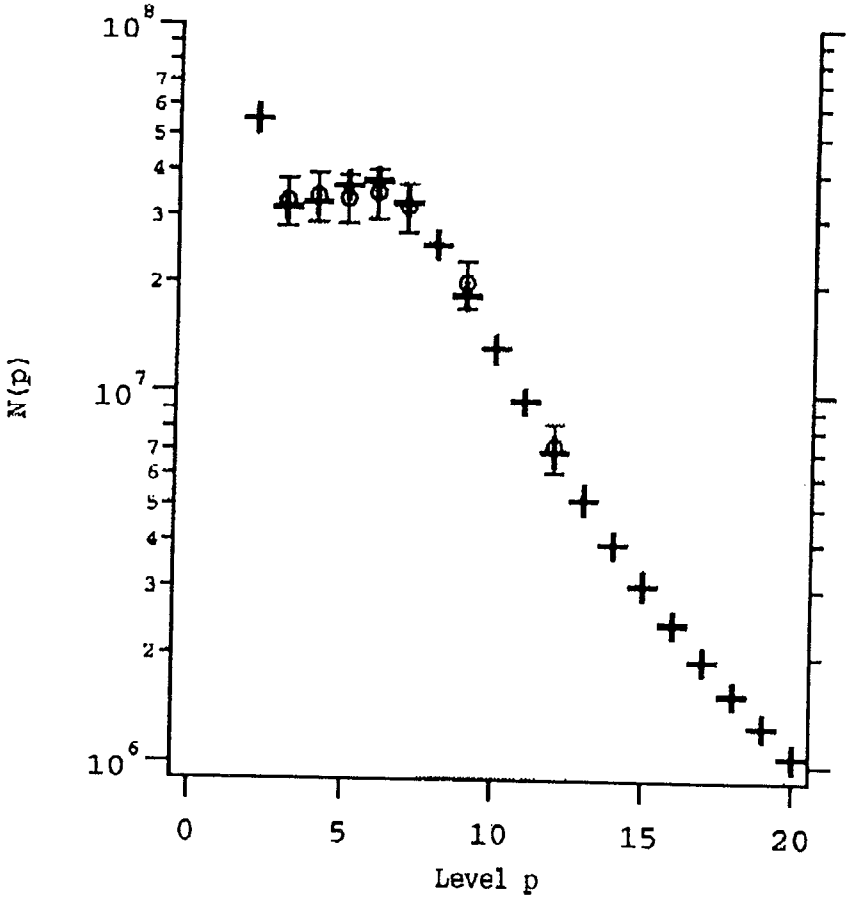

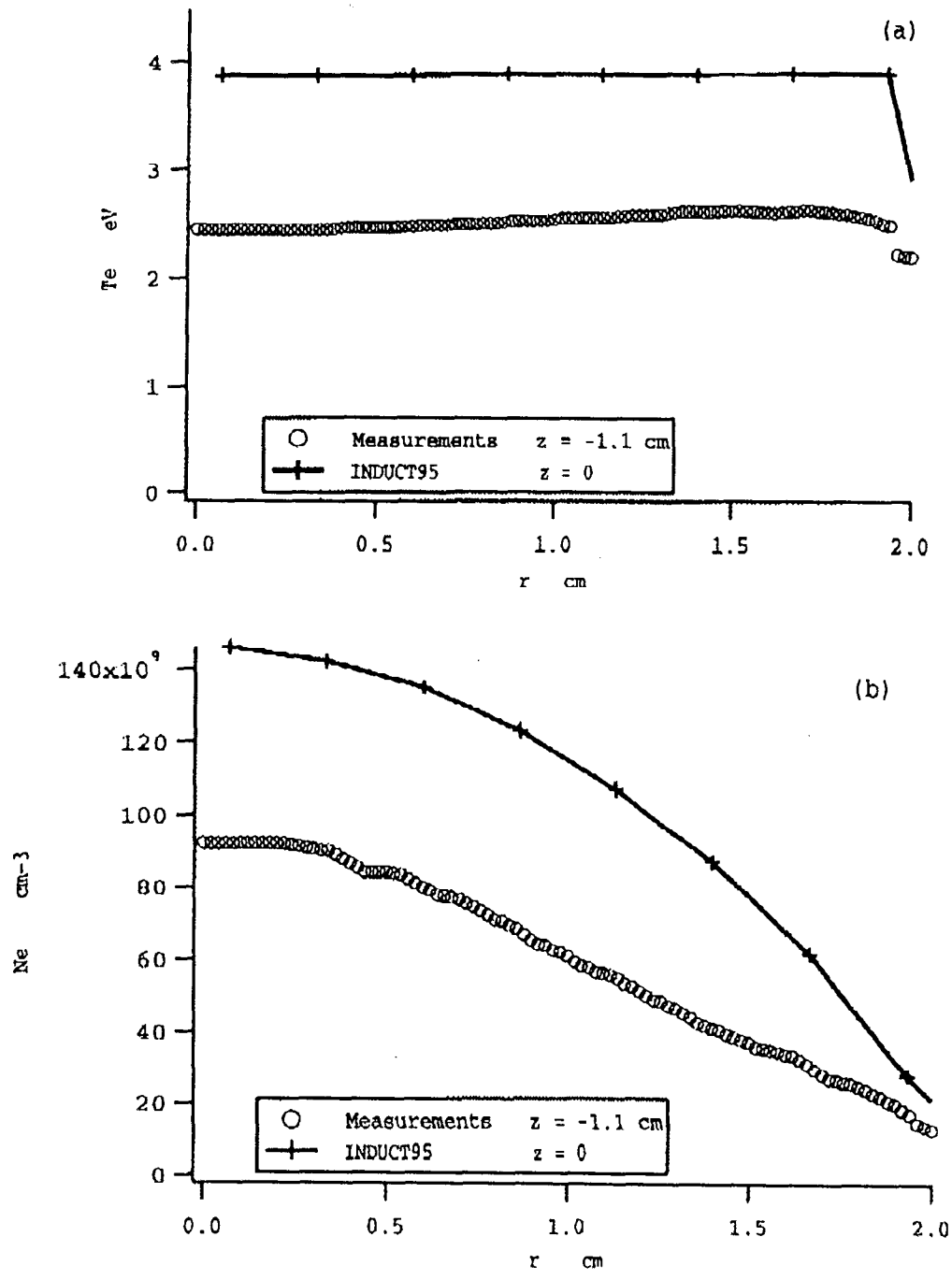
(a)
Te eV
4
3
2
1
0
Measurements z = -1.1 cm
INDUCT95 z = 0
0.0
0.5
1.0
1.5
2.0
r cm
(b)
Ne cm-3
140x10^9
120
100
80
60
40
20
0
Measurements z = -1.1 cm
INDUCT95 z = 0
0.0
0.5
1.0
1.5
2.0
r cm

Figure 2

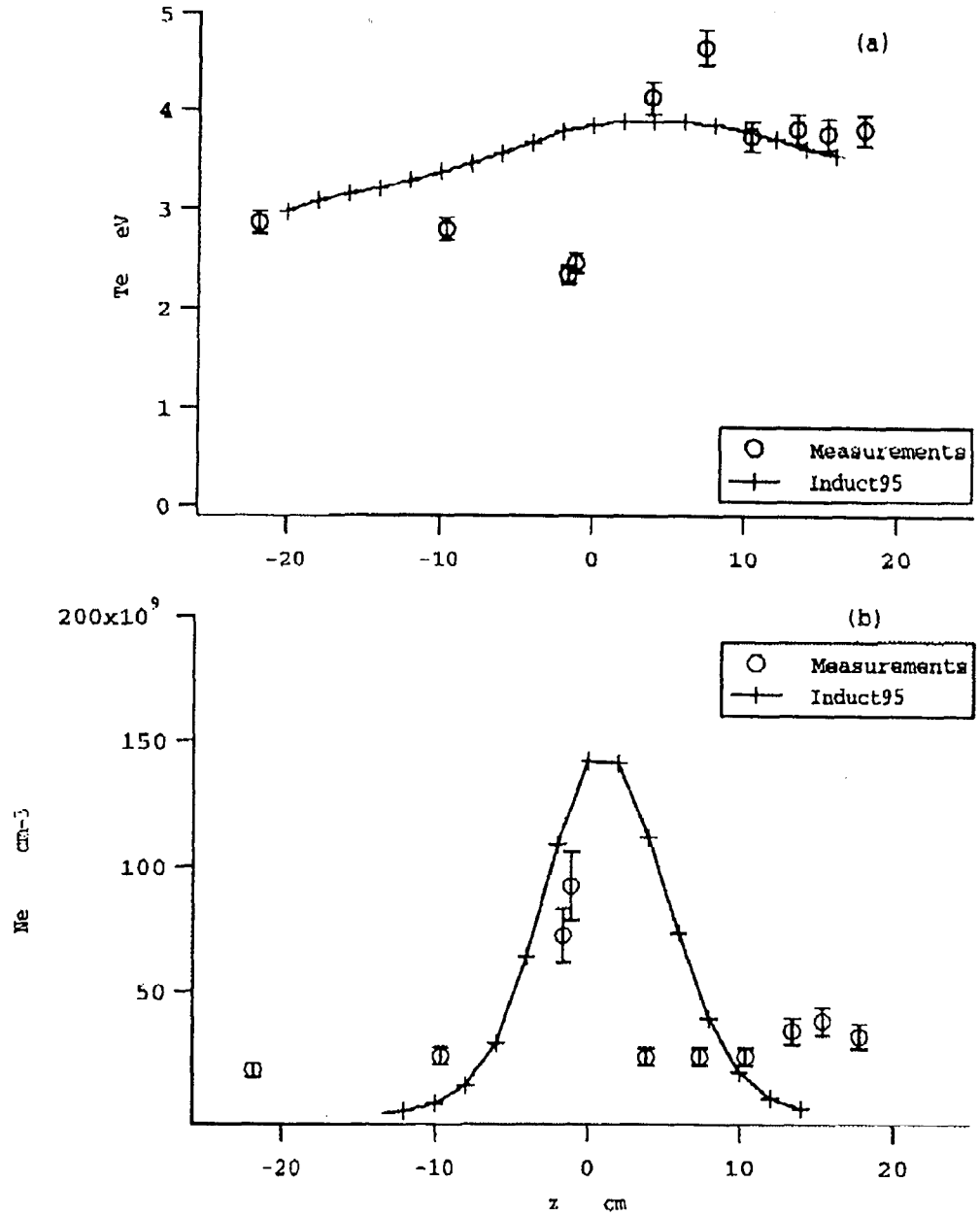
(a)
Te eV
Measurements
Induct95
(b)
Ne cm-3
200x10^9
150
100
50
-20
-10
0
10
20
z cm

Figure 3

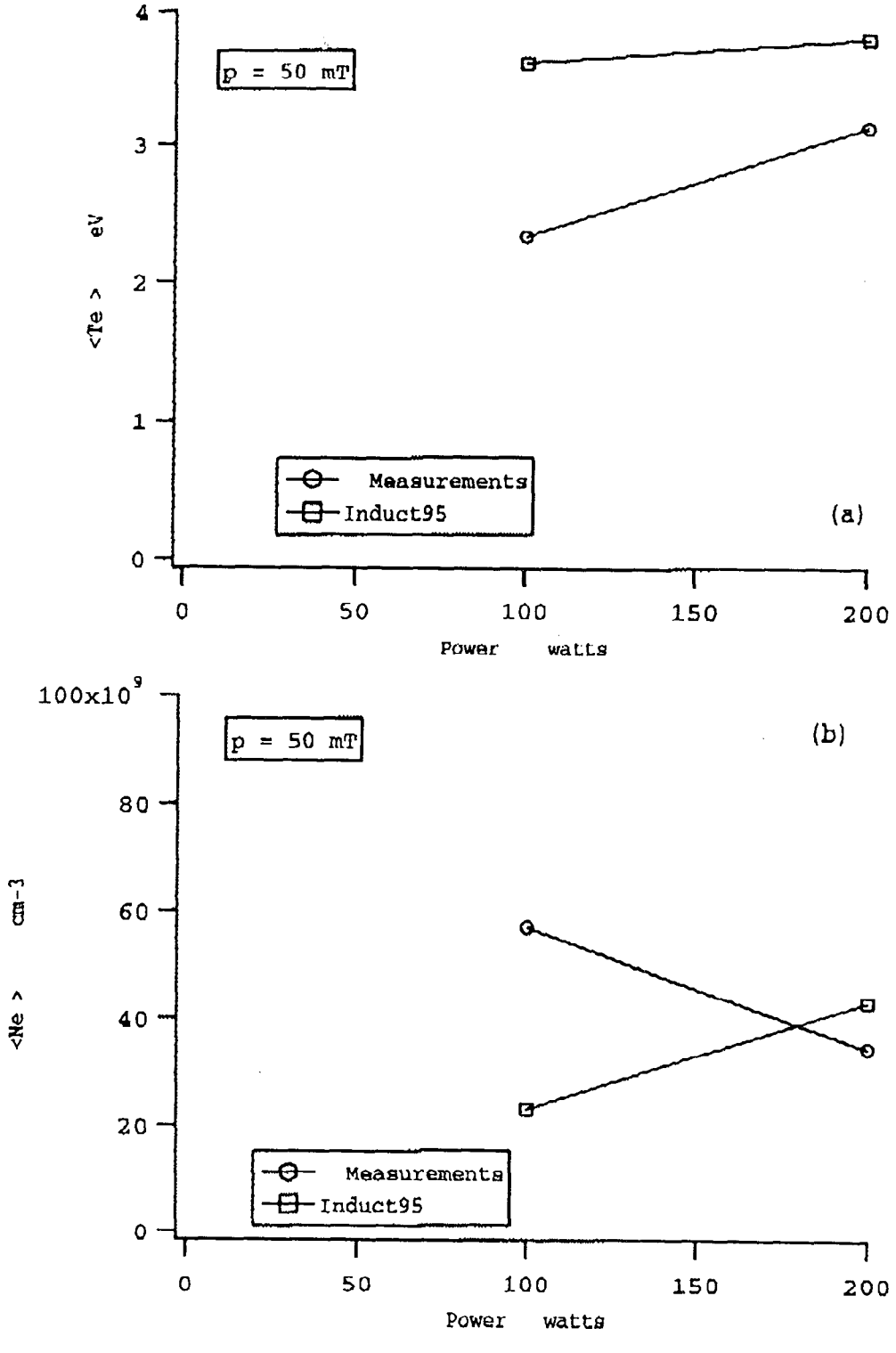
p = 50 mT
<Te > eV
Measurements
Induct95
(a)
Power watts
100x10^9
p = 50 mT
(b)
<Ne > cm-3
Measurements
Induct95
Power watts

Figure 4

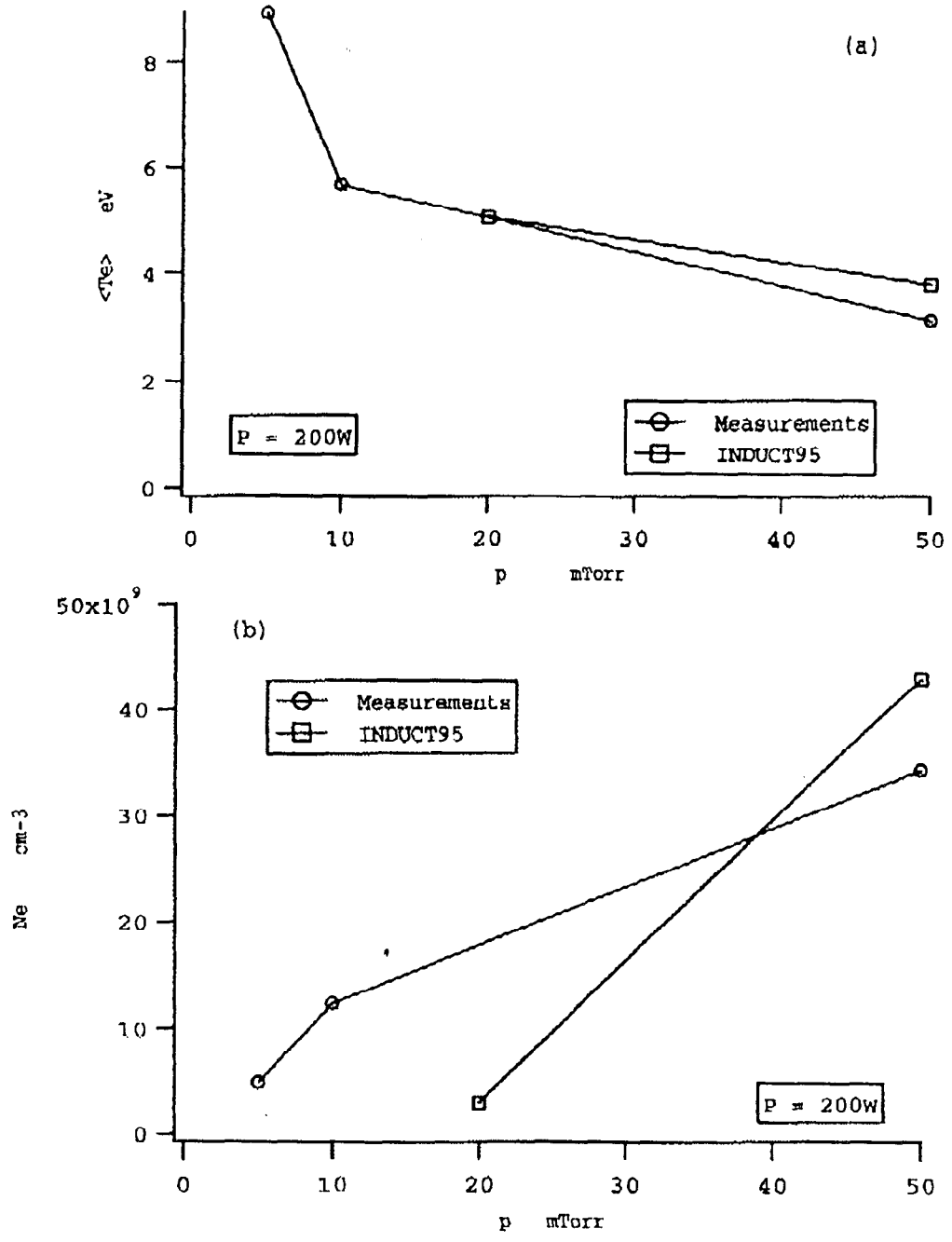
(a)
<Te> eV
8
6
4
2
0
P = 200W
Measurements
INDUCT95
0
10
20
30
40
50
p mTorr
50x10^9
(b)
Measurements
INDUCT95
Ne cm-3
40
30
20
10
0
P = 200W
0
10
20
30
40
50
p mTorr

Figure 5

TABLE 1. Reactions used in INDUCT simulations and source for rates.

Reaction	Source
$e + H \longrightarrow H^+ + e + e$	Sawada
$e + H \longrightarrow H + e$	Lieberman
$e + H \longrightarrow H^* + e$	Sawada
$e + H^+ \longrightarrow H$	Sawada
$e + H_2 \longrightarrow H_2^+ + e + e$	Sawada
$e + H_2 \longrightarrow H_2 + e$	Lieberman
$e + H_2 \longrightarrow H + H + e$	Sawada
$e + H_2 \longrightarrow H + H^+ + e + e$	Sawada
$e + H_2 \longrightarrow H + H^* + e$	Sawada
$e + H_2^+ \longrightarrow H_2$	Sawada
$e + H_2^+ \longrightarrow H + H^* + e$	Janev
$e + H_2^+ \longrightarrow H^+ + H^+ + e + e$	Janev
$H_2 + H_2^+ \longrightarrow H + H_3^+$	Chan et al
$e + H_3^+ \longrightarrow H + H + H$	Janev
$e + H_3^+ \longrightarrow 2H + H^+ + e$	Janev

TABLE II. Wall reactions and wall coefficients used in INDUCT-95 simulations.

Wall reaction	Wall coefficient
$H + wall \longrightarrow 1/2\ H_2$	0.002
$H^+ + wall \longrightarrow wall\ charge + H$	1
$H_2^+ + wall \longrightarrow wall\ charge + H_2$	1
$H_3^+ + wall \longrightarrow wall\ charge + 3/2\ H_2$	1
$e + Wall \longrightarrow wall\ charge$	